

# Orthogonal Protein-Responsive mRNA Switches for Mammalian Synthetic Biology

Hiroki Ono,<sup>†,‡,§</sup> Shunsuke Kawasaki,<sup>†,§</sup> and Hirohide Saito<sup>\*,†,‡</sup>

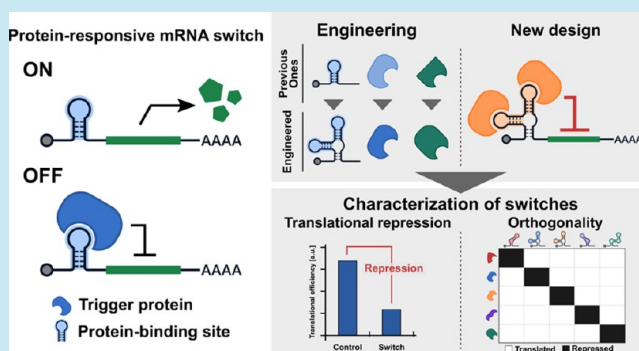
<sup>†</sup>Department of Life Science Frontiers, Center for iPS Cell Research and Application, Kyoto University, 53 Kawahara-cho, Shogoin, Sakyo-ku, Kyoto 606-8507, Japan

<sup>‡</sup>Graduate School of Medicine, Kyoto University, Kyoto 606-8507, Japan

## Supporting Information

**ABSTRACT:** The lack of available genetic modules is a fundamental issue in mammalian synthetic biology. Especially, the variety of genetic parts for translational control are limited. Here we report a new set of synthetic mRNA-based translational switches by engineering RNA-binding proteins (RBPs) and RBP-binding RNA motifs (aptamers) that perform strong translational repression. We redesigned the RNA motifs with RNA scaffolds and improved the efficiency of the repression to target RBPs. Using new and previously reported mRNA switches, we demonstrated that the orthogonality of translational regulation was ensured among five different RBP-responsive switches. Moreover, the new switches functioned not only with plasmid introduction, but also with RNA-only delivery, which provides a transient and safer regulation of expression. The translational regulators using RNA–protein interactions provide an alternative strategy to construct complex genetic circuits for future cell engineering and therapeutics.

**KEYWORDS:** mammalian synthetic biology, gene switch, RNA switch, RNA–protein interaction, translation, aptamer



Synthetic biologists have been developing gene regulatory parts and devices by redesigning natural regulatory elements.<sup>1</sup> Recent progress has expanded the variety of available devices that control gene expressions at multiple steps including transcriptional, translational, and post-translational levels.<sup>2–4</sup> These devices can be modularly assembled to construct complex genetic circuits that realize a more sophisticated, precise regulation of gene expressions and cellular behaviors.<sup>3,5</sup> The attractive features of synthetic devices and circuits will improve the performance and safety of gene therapy and engineered-cell therapy.<sup>3,6</sup>

RNA-based translational regulators have been used to increase the design capability and multilayer capacity of synthetic gene networks.<sup>7,8</sup> Messenger RNAs (mRNAs) that have a specific protein-binding motif (aptamer) in the 5'-UTR (i.e., protein-responsive mRNA switches) serve as powerful components of genetic circuits for the following reasons. First, mRNA switches can respond to target proteins and repress or activate the translation of reporter genes through RNA–protein (RNP) interactions.<sup>9–14</sup> This feature is a strong advantage for scaling up the circuits because the output protein from one mRNA can serve as the input protein of other circuits.<sup>7,8</sup> Second, mRNA switches can be implemented in a variety of vectors, including plasmid DNAs, *in vitro* transcribed RNAs, and self-replicating RNAs.<sup>8</sup> These facts suggest that multilevel control can be implemented in future genetic

circuits by combining different mRNA switches. Additionally, an RNA-only delivery approach may provide a safer means to control cell behavior because synthetic RNA has virtually no risk of genomic damage, whereas DNA-delivered circuits have the potential risk of harmful integration into genomic DNA.<sup>8</sup> Despite such advantages, available RNP interactions and mRNA switches for mammalian synthetic biology are limited. Here we aimed to expand the repertoire of practical mRNA switches in mammalian cells.

We first improved the mRNA switch that responds to MS2 bacteriophage coat protein (MS2CP), a well-characterized RNA-binding protein (RBP) and frequently used as a translational repressor.<sup>2,8,12,15</sup> Previous studies suggest that the stability of the secondary structure of an RNA aptamer in mRNA is an important factor for efficient translational repression.<sup>9,10</sup> It has also been suggested that the insertion of double-stranded scaffold linkers between two RNA stem-loop motifs may stabilize the motifs.<sup>16,17</sup> Thus, we hypothesized that the sensitivity of the mRNA to the target RBP may be improved by embedding the RNA aptamer into a stable RNA scaffold. We designed an aptamer-scaffold (scMS2(WTx2)), which includes two MS2-binding stem-loop motifs (MS2SL), and inserted it into the 5'-UTR of mRNA. To validate the

Received: August 27, 2019

Published: November 25, 2019

effect of the scaffold, we compared the efficiency of translational repression between the scaffold-containing mRNA and previously designed MS2SL-containing mRNAs (MS2SLx1 or MS2SLx2)<sup>12</sup> (Figure 1A, see also secondary

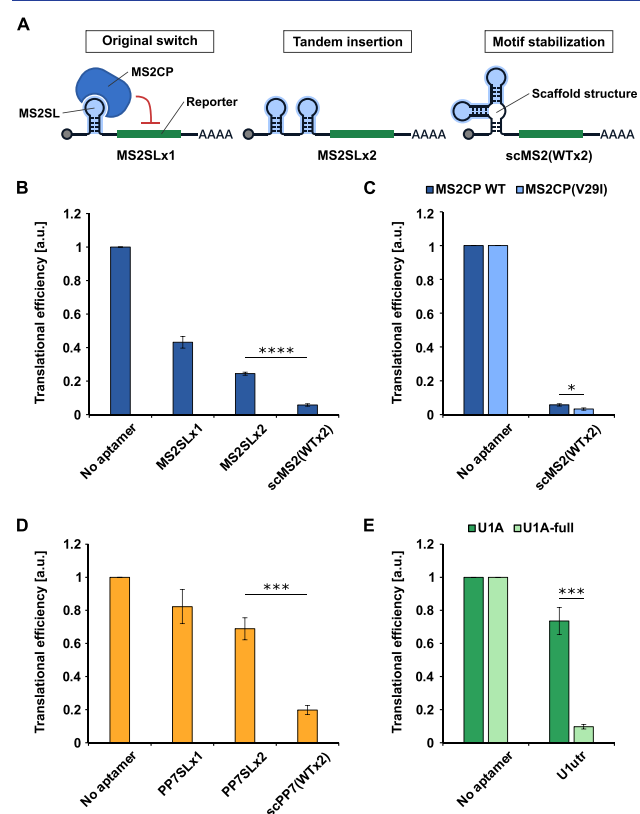


**Figure 1.** Characterization of engineered protein-responsive mRNA switches. (A) Schematic representation of protein-responsive mRNA switches. Here we show the MS2CP-responsive switches as a representative case. Protein-responsive mRNA switches have specific aptamers (colored in light blue) in the 5'-UTR. The translation of protein-responsive mRNA switches is repressed in the presence of trigger proteins via protein-aptamer interactions. We first tested MS2CP-responsive mRNA switches that contain a single aptamer (MS2SLx1), two aptamers (MS2SLx2), or two aptamers embedded in the scaffold (scMS2(WTx2)) in the 5'-UTR. (B) Translational efficiencies of MS2CP-responsive mRNA switches. All values were normalized by cells transfected with a reporter plasmid lacking the aptamer sequence (No aptamer). Error bars represent mean  $\pm$  SD ( $n = 3$  independent experiments performed on different days). (C) Comparison of translational efficiencies between MS2CP WT and MS2CP(V29I). Error bars represent mean  $\pm$  SD ( $n = 3$  independent experiments performed on different days). (D) Translational efficiencies of PP7CP-responsive mRNA switches. Error bars represent mean  $\pm$  SD ( $n = 3$  independent experiments performed on different days). (E) Comparison of translational efficiencies between truncated U1A and U1A-full. Error bars represent mean  $\pm$  SD ( $n = 3$  independent experiments performed on different days). Levels of significance (unpaired two-tailed Student's  $t$ -test) are denoted as \* $P < 0.05$ , \*\*\* $P < 0.001$ , and \*\*\*\* $P < 0.0001$ . a.u. arbitrary units.

structures predicted by CentroidFold software<sup>18</sup> in Figure S1A–C). We prepared CMV promoter-driven constitutive expression plasmid for mRNA switches (referred to as switch plasmid). The switch plasmids encode mRNA switches that contain MS2SL-motif(s) in the 5'-UTR and enhanced green fluorescent protein (EGFP) as a reporter. The switch plasmid was cotransfected into HEK293FT cells with CMV promoter-

driven MS2CP-expression plasmid (referred to as trigger plasmid). The results indicated that scMS2(WTx2)-EGFP significantly improved the translational repression efficiency (94% repression) compared with single or tandem insertion of MS2SL-motif (57% and 76% repression, respectively) (Figure 1B, Figure S2A). Next, we engineered the trigger MS2CP protein with higher affinity, because it may improve the response of the mRNA switch. A previous study reported that a single amino acid substitution, V29I, in MS2CP improved the affinity to the MS2SL motif.<sup>19</sup> We compared the translational repression efficiency of MS2CP with MS2CP-(V29I) and found that MS2CP(V29I) displays stronger translational repression (97% for MS2CP(V29I) and 94% for WT MS2CP,  $P < 0.05$ ) (Figure 1C, Figure S2B). Together, we designed a highly sensitive, MS2CP-responsive mRNA switch with RNA scaffold and high affinity mutant, MS2CP(V29I), indicating that the RNA scaffold-based strategy may improve the sensitivity of the switch more efficiently than the previous strategy that simply inserted aptamers into the 5'-UTR.

Next, we tested an alternative RNA motif to construct a new translational regulator. We chose PP7 bacteriophage coat protein (PP7CP) and its binding motif (PP7SL).<sup>16</sup> Although PP7CP-responsive translational regulators have been reported in prokaryotic studies,<sup>20,21</sup> they have not been used to construct mRNA switches in mammalian cells. We embedded single or tandem PP7SL, or a scaffold including two PP7SL motifs (referred to as scPP7(WTx2)) in the 5'-UTR (Figure S1D–F). The switch plasmids were introduced with a trigger plasmid into HEK293FT cells, and the cells were analyzed 24 h after transfection. The scaffold-embedded scPP7(WTx2) switch showed obvious translational repression (80% repression), whereas the mRNA with a simple insertion of PP7SL(x1 or x2) did not respond to PP7CP efficiently (Figure 1D, Figure S2C). Thus, we generated a new PP7CP-responsive mRNA switch with PP7SL-RNA scaffold that functions in mammalian cells.

We further investigated whether we could improve the performance of previously reported switches by engineering the trigger protein. A well characterized spliceosome-related RBP, U1A, is often used in synthetic biology.<sup>22,23</sup> In most studies, truncated U1A that retains the N-terminal RNA recognition domain but lacks the C-terminal region containing the nuclear localization signal is used. Thus, full-length U1A (U1A-full) has not been tested sufficiently for its translational repression efficiency. We previously constructed U1A-responsive mRNA switches<sup>10</sup> and found that some of them could respond to endogenous U1A. Thus, we speculated that the overexpression of U1A-full may efficiently repress the translation of the switch. To test this hypothesis, we constructed U1A-full trigger plasmid and transfected it into HEK293FT cells with the switch plasmid (U1utr-EGFP). We found that U1A-full can repress the translation of U1utr-EGFP more efficiently than truncated U1A (90% and 26% repression, respectively) (Figure 1E, Figure S2D). Thus, we propose that U1A-full can be used as an effective translational repressor.

One of the applications of mRNA switches is to use them as components of complex genetic circuits. For this purpose, synthetic switches should have high repression efficiency and minimal crosstalk. Therefore, we validated the orthogonality among the mRNA switches constructed in this study (MS2CP(V29I)-, PP7CP-, and U1A-full-responsive) and in previous studies (L7Ae<sup>12,24</sup> and LIN28A-responsive<sup>10</sup>). The translation from each mRNA was significantly repressed only

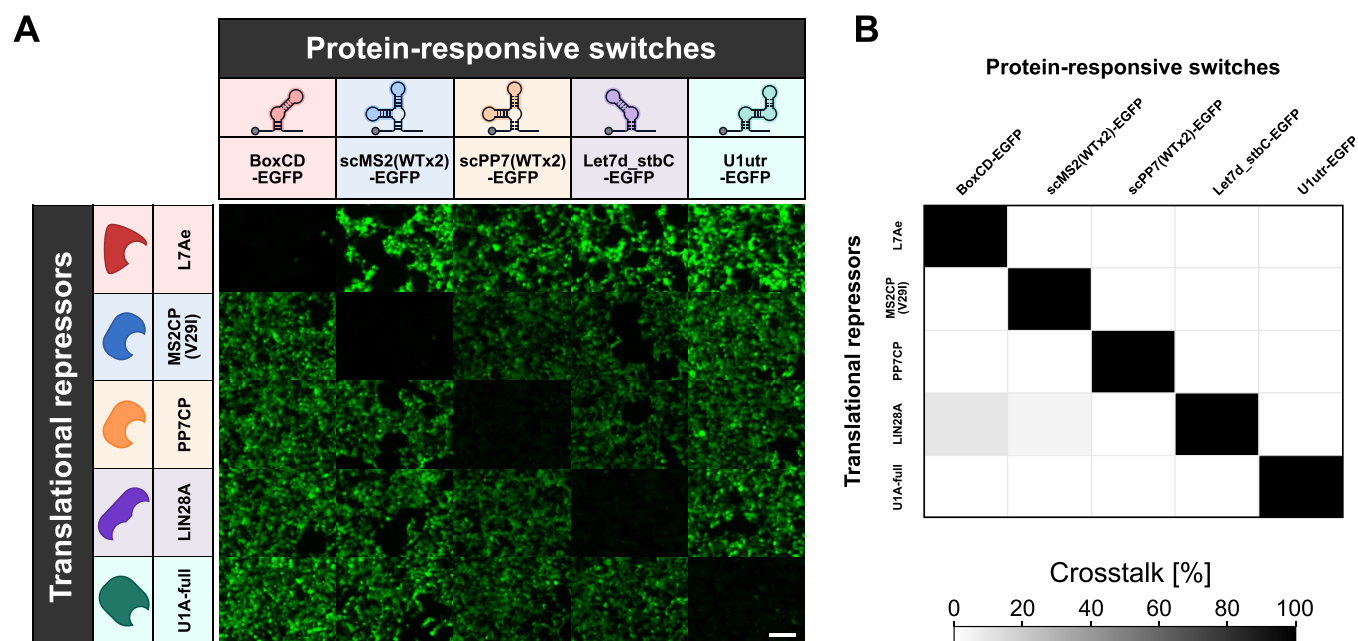


**Figure 2.** Orthogonality among mRNA switches. (A) Representative fluorescent microscopy images of HEK293FT cells transfected with 25 pairwise combination of trigger proteins and mRNA switches. Previously reported switches (L7Ae- and LIN28A-responsive switches) and newly designed switches (MS2-, PP7-, and U1A-full-responsive switches) were tested for their orthogonality. Each switch plasmid was cotransfected with one of the trigger plasmids into HEK293FT cells, and EGFP expression was observed with fluorescence microscopy 24 h after transfection. (B) The percentage of crosstalk was measured with flow cytometry. See [Materials and Methods](#) to find calculation formula for the value of crosstalk. Data were obtained from three independent experiments performed on different days. BoxCD, L7Ae binding aptamer; Let7d\_stbC, LIN28A binding aptamer. 400 ng of trigger plasmid, 100 ng of switch plasmid and 100 ng reference plasmid (iRFP670-expression) were cotransfected. Representative images from three independent experiments are shown. Scale bar, 200  $\mu\text{m}$ . Quantitative data are shown in [Figure S3](#).

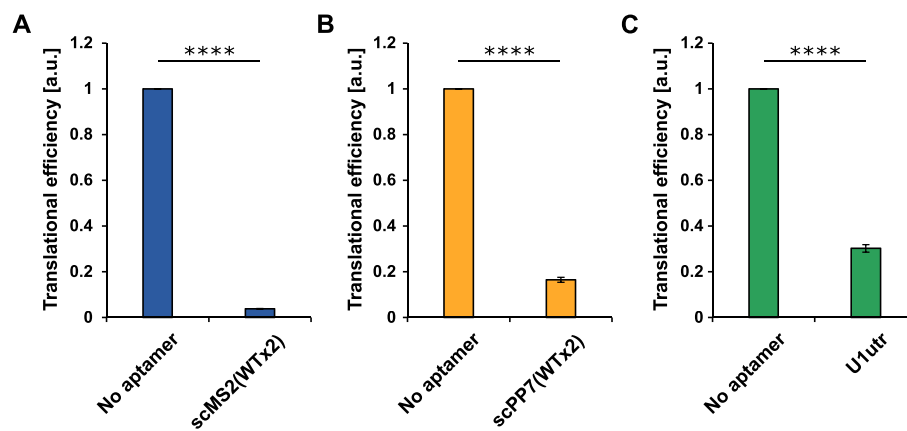


**Figure 3.** Translational efficiencies of *in vitro* transcribed mRNA switches. (A) Translational efficiencies of MS2CP-responsive mRNA switch. (B) Translational efficiencies of PP7CP-responsive mRNA switch. (C) Translational efficiencies of U1A-responsive mRNA switch. All mRNA switches encode EGFP as the reporter. iRFP670-encoding mRNA was cotransfected as a reference. The sequences of the transfected mRNAs are shown in [Supplementary Sequences](#). Error bars represent mean  $\pm$  SD ( $n = 3$  independent experiments performed on different days). The levels of significance (unpaired two-tailed Student's *t*-test) are denoted as \*\*\*\* $P < 0.0001$ . a.u. arbitrary units.

when the appropriate trigger protein was cotransfected ([Figure 2A,B](#)). Notably, no mRNAs had repressed translation obviously when an irrelevant trigger protein was cotransfected ([Figure S3](#)). Although L7Ae induction generally caused higher reporter expression, this effect may be due to the toxicity of excessive L7Ae expression, which may cause the slower cell growth and/or cell death.<sup>25</sup> It would consequently slow down the dilution of cellular components associated with the cell-division, leading to the higher reporter expression in each cell. Taken together,

the tested set of mRNA switches has both high orthogonality and repression efficiency.

Finally, we investigated whether mRNA switches with new RNP modules can function with RNA-only delivery. Recent studies emphasized that synthetic mRNAs and circuits can be delivered with a DNA-free transfection method for future medical applications.<sup>26</sup> We *in vitro* transcribed mRNAs that encode the corresponding aptamer and EGFP as a reporter. We prepared these mRNAs with native bases because the chemical modification might disrupt the RNA secondary structure and RNP interaction. We also prepared trigger



mRNAs that encode the trigger protein (MS2CP(V29I), PP7CP, or U1A-full) and reference iRFP670 mRNA with modified bases. We then cotransfected mRNAs into HEK293FT cells, because HEK293FT cells show attenuated responses to interferon signaling.<sup>10</sup> One day after transfection, we observed significant translational repression (96% repression for MS2CP(V29I), 84% repression for PP7CP, and 70% repression for U1A-full) when the trigger protein-encoded mRNA was cotransfected with the reporter mRNA (Figure 3 and Figure S4). These results indicate that our designed mRNA switches function by RNA-delivery.

It has been reported that the shorter spacer sequence between the RNA motif and the 5'-end of the protein-responsive switches causes higher translational repression.<sup>12</sup> Meanwhile, the presence of a thermostable structure directly behind the cap structure has been reported to inhibit the translation.<sup>27</sup> Given these facts, the position of the stabilized aptamer is a considerable factor for constructing highly sensitive mRNA switches.<sup>10</sup> To investigate this, we tested the positional effect of the RNA motif on the translational repression with the MS2CP-responsive switch. We deleted the spacer sequence from the scMS2(WTx2) switch and placed the motif directly behind the cap structure (this switch is referred to as  $\Delta$ spacer-scMS2(WTx2), Figure S5A). When we compared the translational repression efficiency of the switch with scMS2(WTx2), these switches showed similar efficiency (Figure S5B).  $\Delta$ spacer-scMS2(WTx2) showed lower reporter expression compared with scMS2(WTx2) in both ON and OFF state (Figure S5C). Given that, we should consider the positional effect to make a suitable switch for research purposes, the switch with a higher expression level in ON state or the switch with less leakage in OFF state.

Here we report a set of protein-responsive mRNA switches for mammalian synthetic biology. We improved the translational repression efficiency of two previously reported mRNA switches (97% repression for MS2CP- and 90% repression for U1A-full-responsive) and one newly designed switch (PP7CP-responsive with 80% repression) by redesigning RNA aptamers with an RNA scaffold or engineering trigger proteins (Figure 1). We also tested the orthogonality of five proteins-responsive mRNA switches and found that all showed efficient translational repression and minimal crosstalk (Figure 2). In addition, MS2CP(V29I)-, PP7CP- and U1A-full-responsive mRNA switches were able to function by RNA-delivery (Figure 3). These results indicate that our mRNA switches can function in a variety of vectors and be used to build complex genetic circuits with RNA-delivery approaches.

Synthetic gene circuits composed of RNA-based regulators are promising tools for realizing sophisticated programming of gene expressions and cellular behaviors. Protein-responsive mRNA switches are efficient translational repressors and will provide important genetic components for RNA-based composite circuits. Additionally, expanded mRNA switches can be used for proof-of-concept studies to demonstrate the power of RNA-based complex logic circuits. In previous reports related with multilayered circuits using RNA and RBPs, two RNP modules (L7Ae-BoxCD and MS2CP-MS2SL) were adopted as the processing unit. However, the output gene expression depended on either transcription control via small molecules<sup>7</sup> or translation control via microRNAs,<sup>8</sup> and a complicated circuit in which proteins function as both input and output have not been fully implemented due to the lack of available modules. Recent efforts have attempted to increase

the complexity of post-transcriptional circuits via proteases.<sup>28</sup> Even so, new RNP modules as translational repressors have not progressed satisfactorily. The five orthogonal mRNA switches we characterized in this study can be applied to multiple protein-responsive genetic circuits. Future studies will reveal the design frameworks and methodologies for scalable circuits. Thus, we believe that this report contributes to overcoming the current issues of RNA-based gene circuits and realizing practical biocomputing in mammalian cells.

## MATERIALS AND METHODS

**Plasmid Construction.** The plasmids for switch expression and trigger expression were constructed as previously described.<sup>10</sup> Briefly, single-stranded oligonucleotides encoding aptamer sequences were annealed to generate double-stranded aptamer fragments. The fragments were inserted between the *Bam*HI site and *Age*I site of pAptamerCassette-EGFP. The sequences of the oligonucleotides used to construct switch plasmids are shown in Table S1, and the used plasmids are shown in Table S2.

ORFs of the trigger proteins were amplified by PCR and inserted between the *Sal*I site and *Bam*HI site of pTAPmyc-2A-tagRFP. The primers used to amplify the ORFs are shown in Table S3, and the trigger and reference plasmids used in this study are shown in Table S4.

**mRNA Synthesis.** A template DNA for *in vitro* transcription (IVT) was generated according to methods previously described.<sup>10</sup> Synthetic mRNAs were transcribed by using MEGAscript T7 Transcription Kit (Thermo Fisher Scientific). mRNAs encoding trigger and reference proteins were transcribed with pseudouridine-5'-triphosphate ( $\Psi$ TP) and 5-methylcytidine-5'-triphosphate (m5CTP) (TriLink BioTechnologies) instead of uridine-5'-triphosphate (UTP) and cytosine-5'-triphosphate (CTP), respectively. mRNA switches were transcribed with natural nucleotides (ATP, UTP, GTP, and CTP). The reaction mixtures contained 7.5 mM ATP, 7.5 mM  $\Psi$ TP or UTP, 7.5 mM m5CTP or CTP, 1.5 mM GTP, and 6 mM Anti-Reverse Cap Analog (TriLink BioTechnologies). The reaction mixtures were incubated at 37 °C for 6 h. After the incubation, TURBO DNase (Thermo Fisher Scientific) and Antarctic Phosphatase (New England Biolabs) mixture was added into the reaction mixtures, and the mixtures were incubated at 37 °C for 30 min to 1 h. The transcribed mRNAs were purified using RNeasy MinElute Cleanup Kit (QIAGEN) or Monarch RNA Cleanup Kit (50  $\mu$ g) (New England Biolabs) following the manufacturer's protocols. The primer sets and the template oligo DNA are shown in Table S5, and the template plasmids used for preparing synthetic mRNAs are shown in Table S6.

**Cell Culture.** HEK293FT cells (Invitrogen) were cultured at 37 °C in Dulbecco's modified Eagle's Medium (DMEM) medium (Nacalai tesque) supplemented with 10% fetal bovine serum (FBS) (Biosera, Lot #10259), 2 mM L-Glutamine (Thermo Fisher Scientific), 1X MEM Non-Essential Amino Acids (Thermo Fisher Scientific), and 1 mM Sodium Pyruvate (Sigma) in a humidified atmosphere containing 5% CO<sub>2</sub>.

**Transfection.** Cells were plated into 24-well plates 24 h before transfection. Plasmids were transfected with Lipofectamine 2000 (Thermo Fisher Scientific). Synthetic mRNAs were transfected with Lipofectamine MessengerMax (Thermo Fisher Scientific) following the manufacturer's protocol. The details for each experiment are shown in Table S7.

**Flow Cytometry and Data Analysis.** Transfected cells were analyzed 24 h after transfection. HEK293FT cells were washed with phosphate buffered saline (PBS). Cells were trypsinized with 100  $\mu$ L of 0.25% Trypsin–EDTA (Thermo Fisher Scientific) and incubated at 37 °C for 5 min. After the trypsinization, 100–200  $\mu$ L of fresh medium was added, and the cells were transferred to a fresh microcentrifuge tube passing through a nylon mesh, then analyzed by a BD Accuri C6 flow cytometer (BD Biosciences). EGFP was detected by FL1 (533/30 nm) filters. iRFP670 was detected by FL4 (675/25 nm) filters.

Flow cytometry data sets were analyzed using FlowJo (BD Biosciences) and Excel (Microsoft). Gates were generated by using mock samples. Data from debris were eliminated when preparing forward versus side dot plots (FSC-A versus SSC-A). Then, events on the chart edges in the dot plots of the EGFP intensity versus iRFP670 intensity were removed. In the histogram where iRFP670-intensity is displayed on the X-axis, iRFP670-positive (reference-positive) gate was defined. In the following analysis, the median reporter/reference of each cell was calculated from the reference positive population by FlowJo.

Translational efficiency is defined using the following formulas.

For plasmid transfection experiments,

$$\begin{aligned} \text{normalized intensity (NI)} \\ = 1000 \times \text{median of the ratio (reporter intensity} \\ \text{/reference intensity) of each cell} \end{aligned}$$

For mRNA transfection experiments,

$$\begin{aligned} \text{normalized intensity (NI)} \\ = \text{median of the ratio (reporter intensity} \\ \text{/reference intensity) of each cell} \end{aligned}$$

$$\begin{aligned} \text{relative intensity (RI)} \\ = (\text{NI of trigger} + ) / (\text{NI of trigger} - ) \end{aligned}$$

$$\text{translational efficiency} = (\text{RI}) / (\text{RI of no aptamer sample})$$

All values were normalized by the value of no aptamer sample.

The percentage of crosstalk in Figure 2B was calculated according to the following formula:

For each switch,

$$\begin{aligned} \text{difference} = & (\text{NI of cells transfected in combination with} \\ & \text{each trigger protein}) \\ & - (\text{NI of cells transfected with cognate pair of} \\ & \text{switch and trigger protein}) \end{aligned}$$

$$\begin{aligned} \text{normalized difference} \\ = & (\text{difference of each sample}) \\ & / (\text{difference of no trigger sample}) \end{aligned}$$

$$\begin{aligned} \text{the percentage of crosstalk} \\ = & -100 \times (\text{normalized difference} - 1) \end{aligned}$$

Mean of data from 3 independent experiments were displayed in the heat map (Figure 2B).

**Statistical Analysis.** All bar charts represent mean values and error bars represent standard deviation (SD) from three independent experiments. All statistical analysis was performed by unpaired two-tailed Student's *t*-test using R software. The levels of significance are denoted as \**P* < 0.05, \*\*\**P* < 0.001, \*\*\*\**P* < 0.0001, and n.s., not significant (*P*  $\geq$  0.05).

## ■ ASSOCIATED CONTENT

### 📄 Supporting Information

The Supporting Information is available free of charge at <https://pubs.acs.org/doi/10.1021/acssynbio.9b00343>.

Figure S1: Predicted secondary structures of MS2CP- and PP7CP-responsive switches related to Figure 1; Figure S2: Representative dot plots and histograms related to Figure 1; Figure S3: Translational efficiencies of mRNA switches related to Figure 2; Figure S4: Representative dot plots and histograms related to Figure 3; Figure S5: Positional effect of the translational repression in MS2CP-responsive switch; Table S1: Oligonucleotides used to construct switch plasmids; Table S2: Switch plasmids used in this study; Table S3: Oligonucleotides used to construct trigger plasmids; Table S4: Trigger/reference plasmids used in this study; Table S5: Primers, template oligo DNA for generating synthetic mRNAs; Table S6: Plasmids for generating synthetic mRNAs; Table S7: Transfection tables of all experiments performed in this study; Supplementary Sequences: Sequences of mRNAs used in this study (PDF)

## ■ AUTHOR INFORMATION

### Corresponding Author

\*E-mail: [hirohide.saito@cira.kyoto-u.ac.jp](mailto:hirohide.saito@cira.kyoto-u.ac.jp).

### ORCID

Hirohide Saito: 0000-0002-8570-5784

### Author Contributions

<sup>§</sup>H.O. and S.K. are co-first authors and contributed equally to this work. S.K. conceived the idea. H.O., S.K., and H.S. designed the project. H.O. and S.K. performed the experiments and analyzed the data. H.O., S.K., and H.S. wrote the manuscript.

### Notes

The authors declare no competing financial interest.

## ■ ACKNOWLEDGMENTS

We thank Dr. Kei Endo (The University of Tokyo) and Dr. Peter Karagiannis (Kyoto University) for giving us MS2SL plasmids and critical reading of the manuscript, respectively. We also thank Dr. Yoshihiko Fujita (Kyoto University) for advice and providing the plasmid for the IVT template of iRFP670, Dr. Hideyuki Nakanishi (Kyoto University) for giving iRFP670 expression plasmid and suggestion about use of MS2CP(V29I), and Miho Nishimura for her administrative support. This work was supported by JSPS KAKENHI Grant Number JP 19K16110 (to S.K.), 19J21199 (to H.O.), and 15H05722 (to H.S.).

## REFERENCES

- (1) Bashor, C. J., Horwitz, A. A., Peisajovich, S. G., and Lim, W. A. (2010) Rewiring Cells: Synthetic Biology as a Tool to Interrogate the Organizational Principles of Living Systems. *Annu. Rev. Biophys.* 39, 515–537.
- (2) Ausländer, S., and Fussenegger, M. (2013) From gene switches to mammalian designer cells: Present and future prospects. *Trends Biotechnol.* 31, 155–167.
- (3) Xie, M., and Fussenegger, M. (2018) Designing cell function: assembly of synthetic gene circuits for cell biology applications. *Nat. Rev. Mol. Cell Biol.* 19, 507–525.
- (4) Wang, Y.-H., Wei, K. Y., and Smolke, C. D. (2013) Synthetic Biology: Advancing the Design of Diverse Genetic Systems. *Annu. Rev. Chem. Biomol. Eng.* 4, 69–102.
- (5) Kitada, T., DiAndreth, B., Teague, B., and Weiss, R. (2018) Programming gene and engineered-cell therapies with synthetic biology. *Science* 359, eaad1067.
- (6) Sedlmayer, F., Aubel, D., and Fussenegger, M. (2018) Synthetic gene circuits for the detection, elimination and prevention of disease. *Nat. Biomed. Eng.* 2, 399–415.
- (7) Ausländer, S., Ausländer, D., Müller, M., Wieland, M., and Fussenegger, M. (2012) Programmable single-cell mammalian biocomputers. *Nature* 487, 123–7.
- (8) Wroblewska, L., Kitada, T., Endo, K., Siciliano, V., Stillo, B., Saito, H., and Weiss, R. (2015) Mammalian synthetic circuits with RNA binding proteins for RNA-only delivery. *Nat. Biotechnol.* 33, 839–41.
- (9) Sudrik, C., Arha, M., Cao, J., Schaffer, D. V., and Kane, R. S. (2013) Translational repression using BIV Tat peptide-TAR RNA interaction in mammalian cells. *Chem. Commun.* 49, 7457–7459.
- (10) Kawasaki, S., Fujita, Y., Nagaike, T., Tomita, K., and Saito, H. (2017) Synthetic mRNA devices that detect endogenous proteins and distinguish mammalian cells. *Nucleic Acids Res.* 45, e117–e117.
- (11) Saito, H., Kobayashi, T., Hara, T., Fujita, Y., Hayashi, K., Furushima, R., and Inoue, T. (2010) Synthetic translational regulation by an L7Ae-kink-turn RNP switch. *Nat. Chem. Biol.* 6, 71–78.
- (12) Endo, K., Stapleton, J. A., Hayashi, K., Saito, H., and Inoue, T. (2013) Quantitative and simultaneous translational control of distinct mammalian mRNAs. *Nucleic Acids Res.* 41, e135.
- (13) Endo, K., Hayashi, K., Inoue, T., and Saito, H. (2013) A versatile cis-acting inverter module for synthetic translational switches. *Nat. Commun.* 4, 2393.
- (14) Mol, A. A., Groher, F., Schreiber, B., Rühmkorff, C., and Suess, B. (2019) Robust gene expression control in human cells with a novel universal TetR aptamer splicing module. *Nucleic Acids Res.* 47, e132.
- (15) Stripecke, R., Oliveira, C. C., McCarthy, J. E., and Hentze, M. W. (1994) Proteins binding to 5' untranslated region sites: a general mechanism for translational regulation of mRNAs in human and yeast cells. *Mol. Cell Biol.* 14, 5898–909.
- (16) Zalatan, J. G., Lee, M. E., Almeida, R., Gilbert, L. A., Whitehead, E. H., La Russa, M., Tsai, J. C., Weissman, J. S., Dueber, J. E., Qi, L. S., and Lim, W. A. (2015) Engineering complex synthetic transcriptional programs with CRISPR RNA scaffolds. *Cell* 160, 339–350.
- (17) Matsuura, S., Ono, H., Kawasaki, S., Kuang, Y., Fujita, Y., and Saito, H. (2018) Synthetic RNA-based logic computation in mammalian cells. *Nat. Commun.* 9, 4847.
- (18) Sato, K., Hamada, M., Asai, K., and Mituyama, T. (2009) CentroidFold: A web server for RNA secondary structure prediction. *Nucleic Acids Res.* 37, 277–280.
- (19) Lim, F., and David, S. P. (1994) Mutations that increase the affinity of a translational repressor for RNA. *Nucleic Acids Res.* 22, 3748–3752.
- (20) Katz, N., Kaufmann, B., Cohen, R., Solomon, O., Atar, O., Yakhini, Z., Goldberg, S., and Amit, R. (2017) Synthetic protein-sensing riboswitches. *bioRxiv*, DOI: 10.1101/174888.
- (21) Katz, N., Cohen, R., Solomon, O., Kaufmann, B., Atar, O., Yakhini, Z., Goldberg, S., and Amit, R. (2018) An in Vivo Binding Assay for RNA-Binding Proteins Based on Repression of a Reporter Gene. *ACS Synth. Biol.* 7, 2765–2774.
- (22) Ausländer, S., Stücheli, P., Rehm, C., Ausländer, D., Hartig, J. S., and Fussenegger, M. (2014) A general design strategy for protein-responsive riboswitches in mammalian cells. *Nat. Methods* 11, 1154–60.
- (23) Kashida, S., Inoue, T., and Saito, H. (2012) Three-dimensionally designed protein-responsive RNA devices for cell signaling regulation. *Nucleic Acids Res.* 40, 9369–9378.
- (24) Saito, H., Fujita, Y., Kashida, S., Hayashi, K., and Inoue, T. (2011) Synthetic human cell fate regulation by protein-driven RNA switches. *Nat. Commun.* 2, 160.
- (25) Wagner, T. E., Becraft, J. R., Bodner, K., Teague, B., Zhang, X., Woo, A., Porter, E., Albuquerque, B., Dobosh, B., Andries, O., Sanders, N. N., Beal, J., Densmore, D., Kitada, T., and Weiss, R. (2018) Small-molecule-based regulation of RNA-delivered circuits in mammalian cells. *Nat. Chem. Biol.* 14, 1043–1050.
- (26) Andries, O., Kitada, T., Bodner, K., Sanders, N. N., and Weiss, R. (2015) Synthetic biology devices and circuits for RNA-based “smart vaccines”: A propositional review. *Expert Rev. Vaccines* 14, 313–331.
- (27) Babendure, J. R. (2006) Control of mammalian translation by mRNA structure near caps. *RNA* 12, 851–861.
- (28) Cella, F., Wroblewska, L., Weiss, R., and Siciliano, V. (2018) Engineering protein-protein devices for multilayered regulation of mRNA translation using orthogonal proteases in mammalian cells. *Nat. Commun.* 9, 4392.

## SUPPLEMENTARY INFORMATION

Orthogonal Protein-Responsive mRNA Switches for Mammalian Synthetic Biology

Hiroki Ono<sup>1,2,3</sup>, Shunsuke Kawasaki<sup>1,3</sup>, Hirohide Saito<sup>1\*</sup>

<sup>1</sup>Department of Life Science Frontiers, Center for iPS Cell Research and Application, Kyoto University, 53 Kawahara-cho, Shogoin, Sakyo-ku, Kyoto 606-8507, Japan, <sup>2</sup>Graduate School of Medicine, Kyoto University, Kyoto 606-8507, Japan, <sup>3</sup>Co-first author, \*Corresponding author

### Contents

Figure S1. Predicted secondary structures of MS2CP- and PP7CP-responsive switches related to Figure 1

Figure S2. Representative dot plots and histograms related to Figure 1

Figure S3. Translational efficiencies of mRNA switches related to Figure 2

Figure S4. Representative dot plots and histograms related to Figure 3

Figure S5. Positional effect of the translational repression in MS2CP-responsive switch

Table S1. Oligonucleotides used to construct switch plasmids

Table S2. Switch plasmids used in this study

Table S3. Oligonucleotides used to construct trigger plasmids

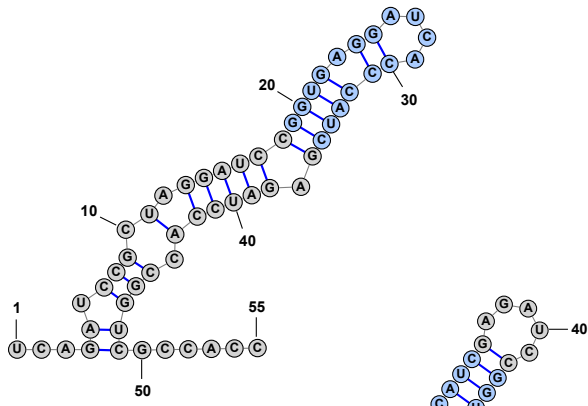
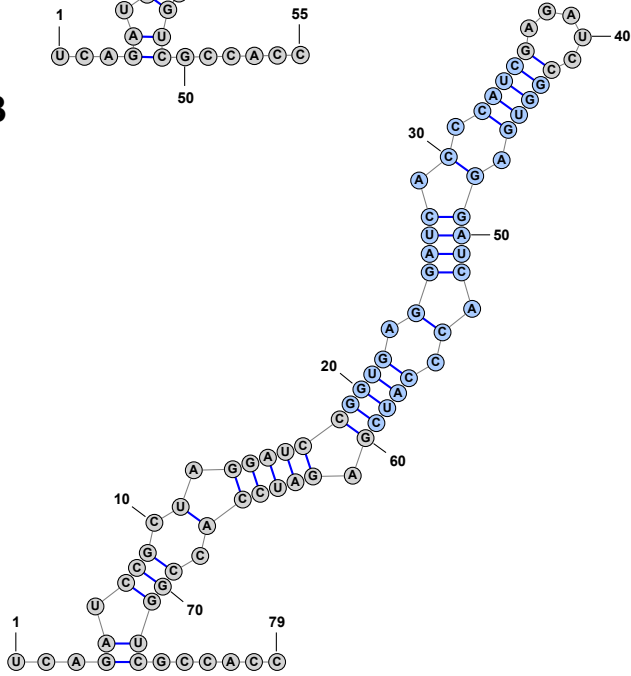
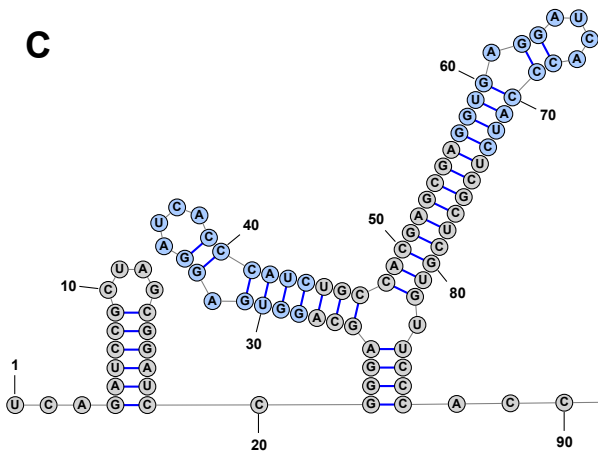
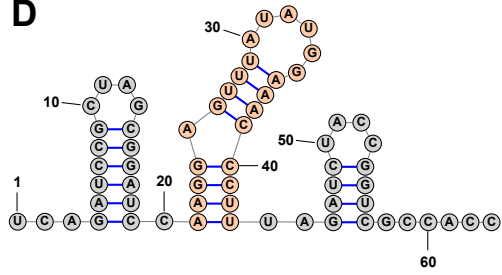
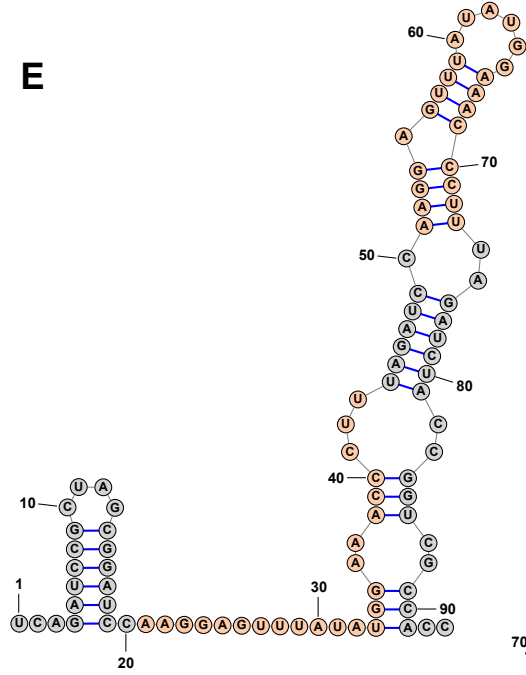
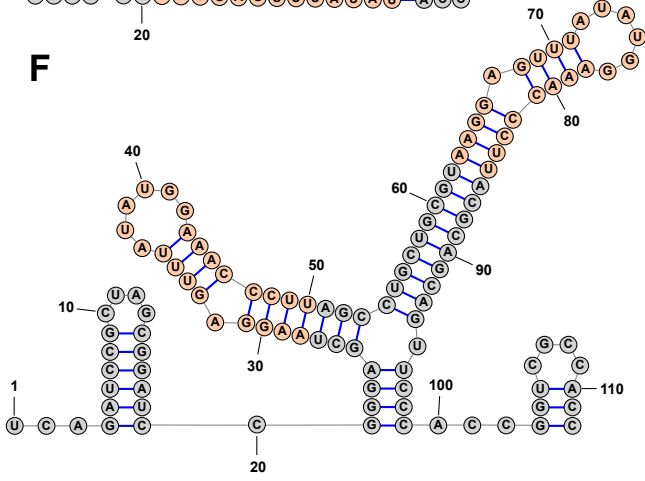
Table S4. Trigger/reference plasmids used in this study

Table S5. Primers, template oligo DNA for generating synthetic mRNAs

Table S6. Plasmids for generating synthetic mRNAs

Table S7. Transfection tables of all experiments performed in this study

Supplementary sequences. Sequences of mRNAs used in this study

**A****B****C****D****E****F**



**Figure S1. Predicted secondary structures of MS2CP- and PP7CP-responsive switches related to Figure 1**

Sequences and the predicted secondary structures of 5'-UTR containing (A) MS2SLx1, (B) MS2SLx2, (C) scMS2(WTx2), (D) PP7SLx1, (E) PP7SLx2, and (F) scPP7(WTx2). Sequences of the 5'-UTR of the switch plasmids are shown. The structures were predicted with CentroidFold software<sup>18</sup>. Sequences shown in blue and orange circles indicate the MS2CP-binding motif and the PP7CP-binding motif, respectively.

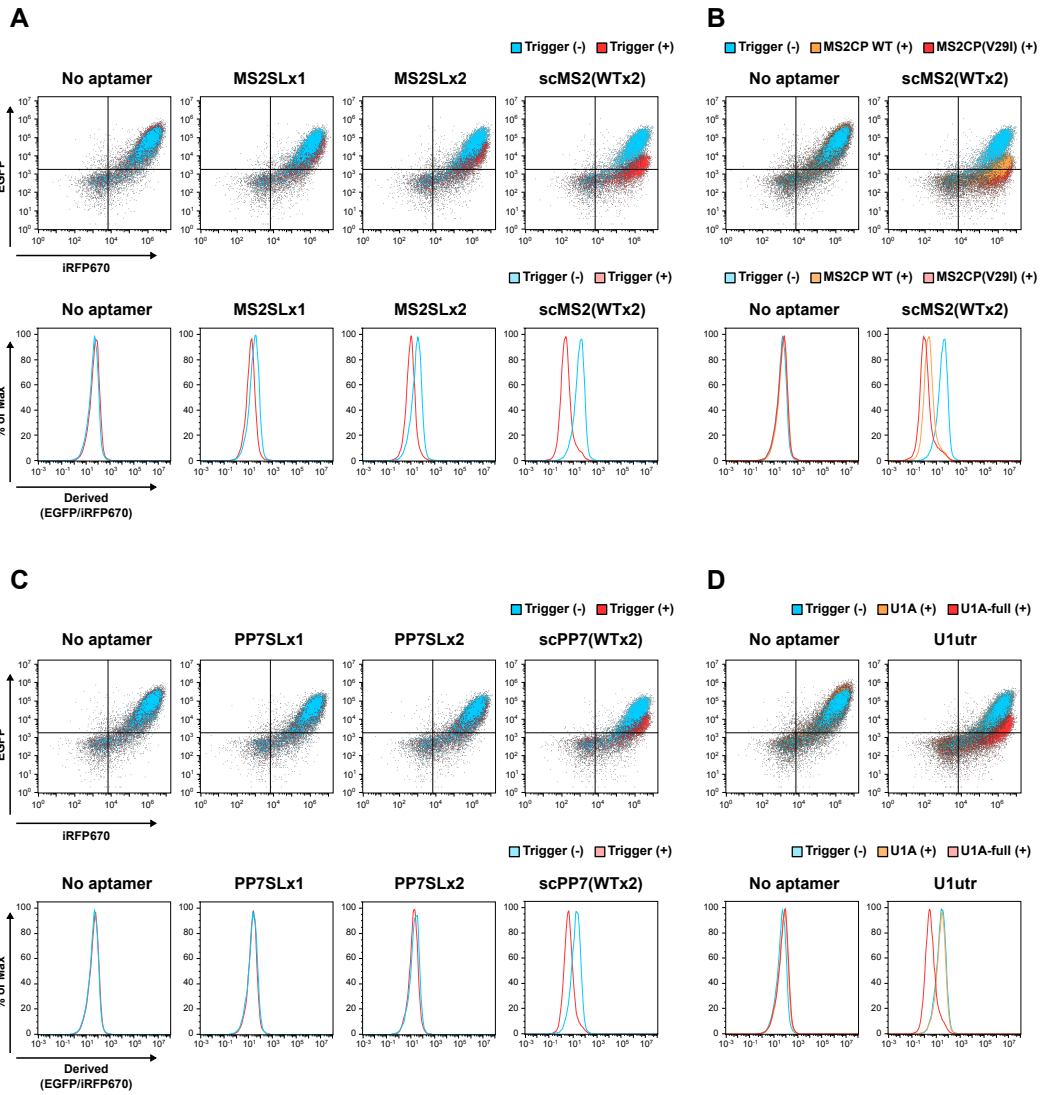


**Figure S2. Representative dot plots and histograms related to Figure 1**

(A) Representative data of MS2CP-responsive mRNA switch related to Figure 1B. Red, cells co-transfected with switch plasmid, trigger plasmid, and iRFP670 plasmid. Blue, cells co-transfected with switch plasmid, control trigger plasmid (pTAPmyc-T2A-tagRFP) and iRFP670 plasmid. Derived values denote EGFP/iRFP670. (B) Representative data of MS2CP-responsive mRNA switch related to Figure 1C. Red, cells co-transfected with switch plasmid, trigger plasmid (MS2CP(V29I)), and iRFP670 plasmid. Orange, cells co-transfected with switch plasmid, trigger plasmid (MS2CP WT), and iRFP670 plasmid. Blue, cells co-transfected with switch plasmid, control trigger plasmid (pTAPmyc-T2A-tagRFP) and iRFP670 plasmid. Derived values denote EGFP/iRFP670. (C) Representative data of PP7CP-responsive mRNA switch related to Figure 1D. Red, cells co-transfected with switch plasmid, trigger plasmid, and iRFP670 plasmid. Blue, cells co-transfected with switch plasmid, control trigger plasmid (pTAPmyc-T2A-tagRFP) and iRFP670 plasmid. Derived values denote EGFP/iRFP670. (D) Representative data of U1A-responsive mRNA switch related to Figure 1E. Red, cells co-transfected with switch plasmid, trigger plasmid (U1A-full), and iRFP670 plasmid. Orange, cells co-transfected with switch plasmid, trigger plasmid (U1A), and iRFP670 plasmid. Blue, cells co-transfected with switch plasmid, control trigger plasmid (pTAPmyc-T2A-tagRFP) and iRFP670 plasmid. Derived values denote EGFP/iRFP670.

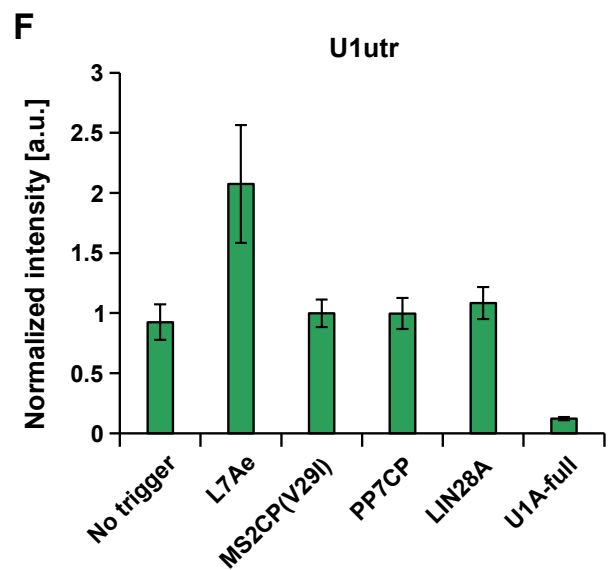
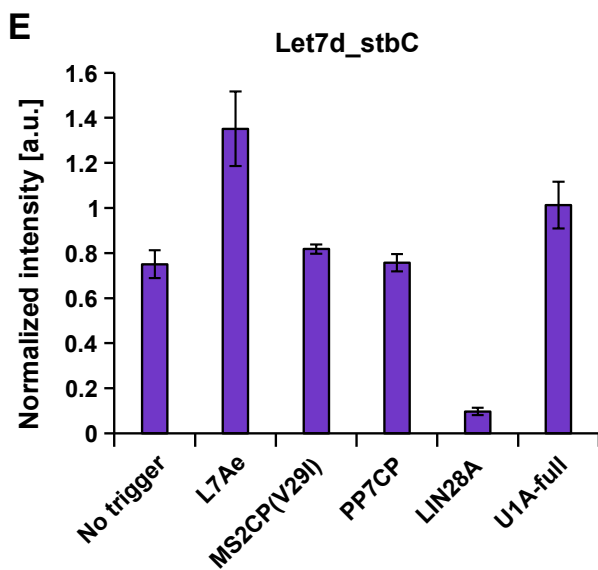
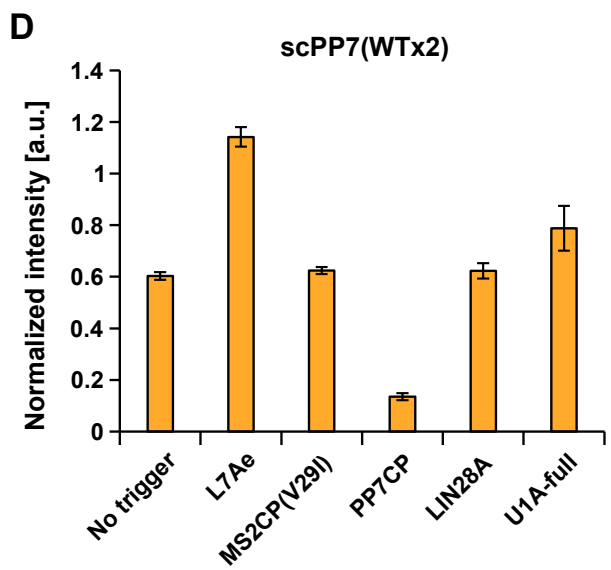
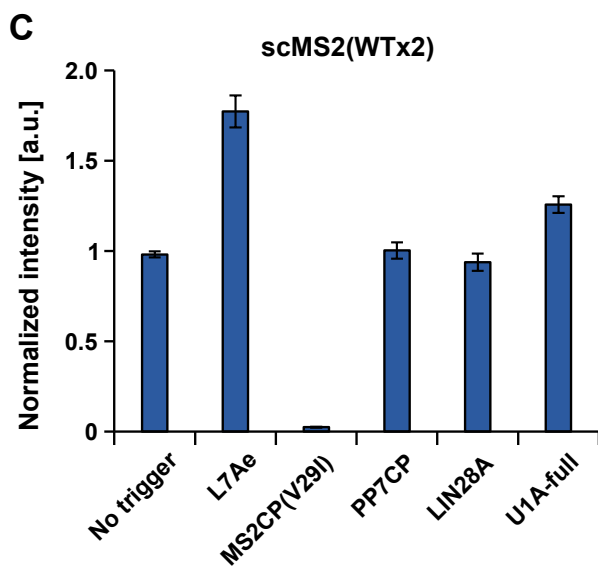
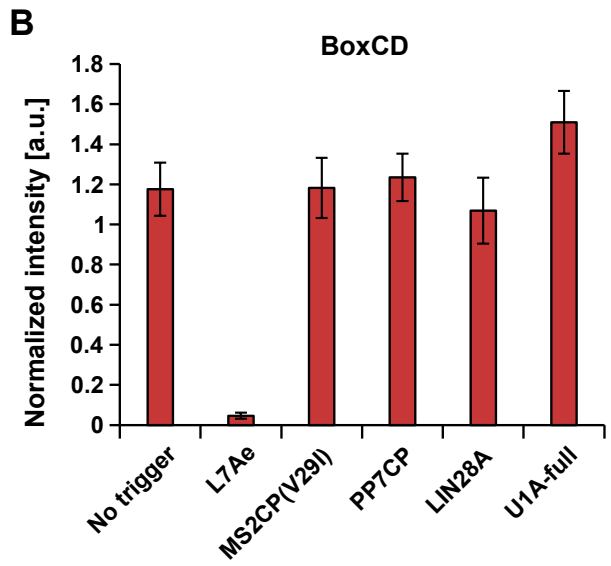
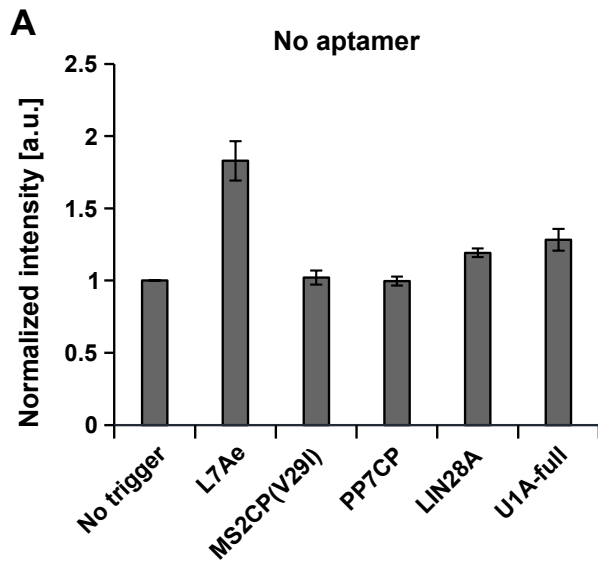




**Figure S3. Translational efficiencies of mRNA switches related to Figure 2**

All values were normalized to cells transfected with control EGFP expression plasmid, which does not encode aptamers, and control trigger plasmid (pTAPmyc-T2A-tagRFP). Error bars represent mean  $\pm$  SD (n = 3 independent experiments performed on different days).

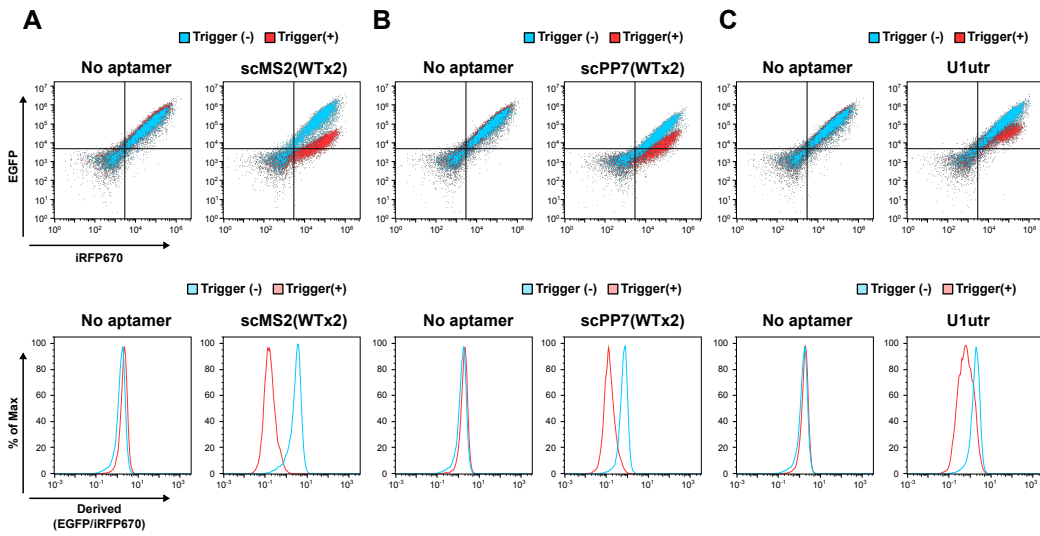


**Figure S4. Representative dot plots and histograms related to Figure 3**

Upper side shows overlaid dot plots and lower side represents histograms from flow cytometry analysis.

(A) Representative data of MS2CP-reponsive mRNA switch.

(B) Representative data of PP7CP-reponsive mRNA switch.

(C) Representative data of U1A-reponsive mRNA switch.

Red, cells co-transfected with switch mRNA, trigger mRNA, and iRFP670 mRNA. Blue, cells co-transfected with switch mRNA and iRFP670 mRNA (without trigger mRNA). Derived values denote EGFP/iRFP670.

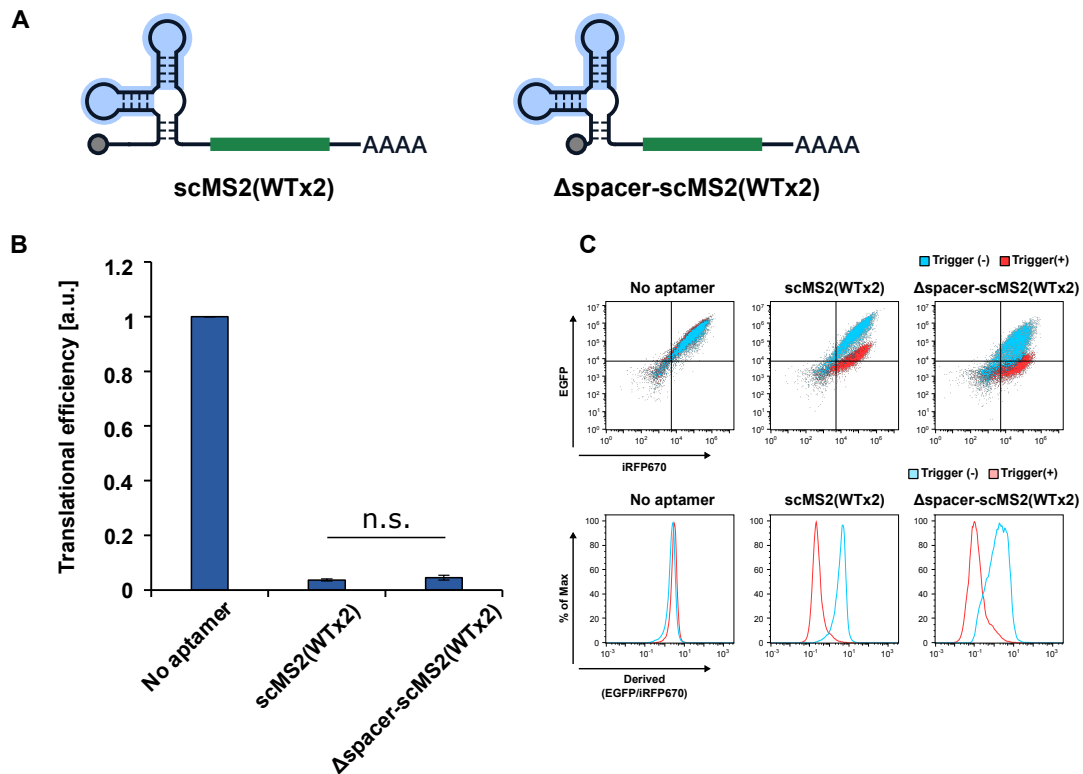


### Figure S5. Positional effect of the translational repression in MS2CP-responsive switch

(A) Schematic representation of the scMS2(WTx2) switch and the  $\Delta$  spacer-scMS2(WTx2) switch. In the latter switch, the RNA motif is placed just behind the cap structure. (B) Comparison of translational efficiencies of the scMS2(WTx2) switch and the  $\Delta$  spacer-scMS2(WTx2) switch. Error bars represent mean  $\pm$  SD ( $n = 3$  independent experiments performed on different days). The levels of significance (unpaired two-tailed Student's  $t$ -test) are denoted as n.s., not significant ( $P \geq 0.05$ ). a.u. arbitrary units. (C) Representative overlaid dot plots and histograms from flow cytometry analysis. Red, cells co-transfected with switch mRNA, trigger mRNA, and iRFP670 mRNA. Blue, cells co-transfected with switch mRNA and iRFP670 mRNA (without trigger mRNA). Derived value denotes EGFP/iRFP670.

**Table S1. Oligonucleotides used to construct switch plasmids**

ID	Name	Sequence (5' -> 3')	Notes
KWC 123	BamHI-scMS2(WTx2)-AgeI_code	GATCCGGGAGCAGGTGAGGATCACCCAT CTGCCACGAGCGAGGTGAGGATCACCCA TCTCGCTCGTGTCCCA	Single-stranded "code" and "temp" oligonucleotides are annealed and inserted into BamHI and AgeI sites of pAptamerCassette-EGFP.
KWC 124	BamHI-scMS2(WTx2)-AgeI_temp	CCGGTGGGAACACGAGCGAGATGGGTGA TCCTCACCTCGCTCGTGGCAGATGGGTG ATCCTCACCTGCTCCCG	Single-stranded "code" and "temp" oligonucleotides are annealed and inserted into BamHI and AgeI sites of pAptamerCassette-EGFP.
KWC 295	PP7SL_code	GATCCAAGGAGTTTATATGGAAACCTT TAGATCTA	Single-stranded "code" and "temp" oligonucleotides are annealed and inserted into BamHI and AgeI sites of pAptamerCassette-EGFP.
KWC 296	PP7SL_temp	CCGGTAGATCTAAAGGGTTCCATATAA ACTCCTTG	Single-stranded "code" and "temp" oligonucleotides are annealed and inserted into BamHI and AgeI sites of pAptamerCassette-EGFP.
KWC 297	PP7SLx2_code	GATCCAAGGAGTTTATATGGAAACCTT TAGATCCAAGGAGTTTATATGGAAACCC TTTAGATCTA	Single-stranded "code" and "temp" oligonucleotides are annealed and inserted into BamHI and AgeI sites of pAptamerCassette-EGFP.
KWC 298	PP7SLx2_temp	CCGGTAGATCTAAAGGGTTCCATATAA ACTCCTTGGATCTAAAGGGTTCCATAT AAACTCCTTG	Single-stranded "code" and "temp" oligonucleotides are annealed and inserted into BamHI and AgeI sites of pAptamerCassette-EGFP.
HKO 57	scPP7(2xWT)_fwd	GATCCGGGAGCTAAGGAGTTTATATGGA AACCTTAGCCTGCTGCGTAAGGAGTTT ATATGGAAACCTTACGCAGCAGTTCCC A	Single-stranded "fwd" and "rev" oligonucleotides are annealed and inserted into BamHI and AgeI sites of pAptamerCassette-EGFP.
HKO 58	scPP7(2xWT)_rev	CCGGTGGGAACCTGCTGCGTAAGGGTTTC CATATAAACTCCTTACGCAGCAGGCTAA GGGTTTCCATATAAACTCCTTAGCTCCC G	Single-stranded "fwd" and "rev" oligonucleotides are annealed and inserted into BamHI and AgeI sites of pAptamerCassette-EGFP.



**Table S2. Switch plasmids used in this study**

Name	Notes	References
pAptamerCassette-EGFP	Double-stranded aptamer fragments were inserted between BamHI and AgeI sites of this plasmid.	10
pMS2SLx1-EGFP	Gift from Dr. Kei Endo.	This study
pMS2SLx2-EGFP	Gift from Dr. Kei Endo.	This study
pscMS2(WTx2)-EGFP	Double stranded scMS2(WTx2) motif was inserted between BamHI and AgeI sites of pAptamerCassette-EGFP.	This study
pPP7SLx1-EGFP	Double stranded PP7SL motif was inserted between BamHI and AgeI sites of pAptamerCassette-EGFP.	This study
pPP7SLx2-EGFP	Double stranded PP7SL motifs were tandemly inserted between BamHI and AgeI sites of pAptamerCassette-EGFP.	This study
pscPP7(2xWT)-EGFP	Double stranded scPP7(WTx2) motif was inserted between BamHI and AgeI sites of pAptamerCassette-EGFP.	This study
pBoxCDGC-KMet-EGFP	Previously reported plasmid.	12
plet7d_stbC-EGFP	Previously reported plasmid.	10
pUltr-EGFP	Previously reported plasmid.	10

**Table S3. Oligonucleotides used to construct trigger plasmids**

ID	Name	Sequence (5' -> 3')	Notes
KWC 117	Xho1-MS2CP-BamH1_Fw	GAGCTCGAGCCCACCATGGCTTCTAACTTTACTCAGTTCG	For amplification of MS2CP ORF to be inserted into pTAPmyc-2A-tagRFP.
KWC 118	Xho1-MS2CP-BamH1_Rv	CTCGGATCCGTAGATGCCGGAGTTGGCCGG	For amplification of MS2CP ORF to be inserted into pTAPmyc-2A-tagRFP.
HKO 67	SalI-kozak-PP7_fwd	ATTGTGACGCCACCATGCTAGCCTCCAAAACC	For amplification of PP7CP ORF to be inserted into pTAPmyc-2A-tagRFP.
HKO 68	BamHI-PP7_rev	ATTGGATCCACGGCCAGCGGCACAAG	For amplification of PP7CP ORF to be inserted into pTAPmyc-2A-tagRFP.
HNC 380	MS2CP_V29I_m utF	ATCGCTGAATGGATCAGCTCTAACTC	For introducing a point mutation in MS2CP ORF to generate MS2CP(V29I).
HNC 381	MS2CP_V29I_m utR	CCCGTTAGCGAAGTTGCTTGG	For introducing a point mutation in MS2CP ORF to generate MS2CP(V29I).
KWC 025	SalI-U1A full-BamH1_Fw	GAGGTCGACACCATGGCGGCAGTTCGCCGAGACC	For amplification of U1A-full ORF to be inserted into pTAPmyc-2A-tagRFP.
KWC 026	SalI-U1A full-BamH1_Rv	CTCGGATCCCTTCTTGCAAAGGAGATCTTCATGGC	For amplification of U1A-full ORF to be inserted into pTAPmyc-2A-tagRFP.
KWC 054	SalI-L7KK-Bgl2_Fw	GAGGTCGACCCCACCATGTACGTGAGATTTGAGGTTCCCTGAGGACATG	For amplification of L7Ae ORF to be inserted into pTAPmyc-2A-tagRFP.
KWC 116	SalI-L7-BamH1_Rv	CTCGGATCCCTTCTGAAGGCCTTTAATCTTCTCC	For amplification of L7Ae ORF to be inserted into pTAPmyc-2A-tagRFP.

**Table S4. Trigger/reference plasmids used in this study**

Name	Notes	Source
pTAPmyc-T2A-tagRFP	ORFs of trigger proteins were inserted between SalI and BamHI sites of this plasmid.	10
pTrg5H-MS2CP	Template for amplification of MS2CP.	12
PP7_mCherry	Template for amplification of PP7CP.	Addgene, #61763
pTrg5H-L7tap	Template for amplification of L7Ae.	12
pMS2CP-myc-T2A-tagRFP	MS2CP expression plasmid.	This study
pMS2CP(V29I)-myc-T2A-tagRFP	MS2CP(V29I) expression plasmid. Point mutation was introduced with MS2CP_V29I_mutF and MS2CP_V29I_mutR by using KOD-Plus-Mutagenesis Kit (Takara).	This study
pPP7CP-myc-T2A-tagRFP	PP7CP expression plasmid. ORF of PP7CP was inserted into pTAPmyc-T2A-tagRFP.	This study
pU1A-myc-T2A-tagRFP	Truncated U1A expression plasmid.	10
pU1A_full-myc-T2A-tagRFP	U1A-full expression plasmid. ORF of U1A-full was amplified from cDNA of iPS cell (201B7) and inserted into pTAPmyc-T2A-tagRFP.	This study
pL7Ae-myc-T2A-tagRFP	L7Ae expression plasmid.	This study
pLin28A-myc-T2A-tagRFP	LIN28A expression plasmid.	10
pCMV-tdiRFP670	iRFP670 expression plasmid as a transfection control.	Gift from Dr. Nakanishi

**Table S5. Primers, template oligo DNA for generating synthetic mRNAs**

ID	Name	Sequence (5' -> 3')	Notes
KD 1-62	IVT_5prime_UTR	CAGTGAATTGTAATACGACTCACTATAGGGC GAATTAAGAGAGAAAAGAAGAGTAAGAAGAA ATATAAGACACCGGTCGCCACCATG	Template for amplification of 5'-UTR fragment.
SKC-111	TAP_T7_G3C fwd primer	CAGTGAATTGTAATACGACTCACTATAGGGC	Forward primer for amplification of 5'-UTR fragment.
KD 1-1	Rev5UTR	CATGGTGGCGACCGGTGTCTTATATTTCTTC TTRACTC	Reverse primer for amplification of 5'-UTR fragment.
KD 1-63	IVT_3prime_UTR	TCTAGACCTTCTGCGGGGCTTGCCTTCTGGC CATGCCCTTCTTCTCTCCCTTGCACCTGTAC CTCTTGGTCTTTGAATAAAGCCTGAGTAGG	Template for amplification of 3'-UTR fragment.
KD 1-4	Fwd3UTR	TCTAGACCTTCTGCGGGGC	Forward primer for amplification of 3'-UTR fragment.
KD 1-65	Rev3UTR2T20	TTTTTTTTTTTTTTTTTTTTTCTACTCAGGC TTTATTCAAAGACCAAG	Reverse primer for amplification of 3'-UTR fragment.
KEC-883	3UTR120A	TTTTTTTTTTTTTTTTTTTTTTTTTTTTTTTTTT TTTTTTTTTTTTTTTTTTTTTTTTTTTTTTTTTT TTTTTTTTTTTTTTTTTTTTTTTTTTTTTTTTTT TTTTTTTTTTTTTTTTTTTTTTTTTTTTTTTTTT TTTTTTTTTTTTTTTTTTTTTTTTTTTTTTCCTA CTCAGGCTTTATTCA	Reverse primer for generation of IVT template by Fusion PCR. 5'-UTR fragment, ORF fragment, and 3'-UTR fragment are fused by fusion PCR with TAP_T7_G3C fwd primer and this primer.
HNC-365	MS2CP_IVTfwd	CACCGGTCGCCACCATGGCTTCTAACTTTAC	For amplification of MS2CP(V29I) ORF for IVT template.
HNC-379	MS2CP_IVTrev	GCCCCGCAGAAGGTCTAGATTCAGTAGATGC CGGAGTTGG	For amplification of MS2CP(V29I) ORF for IVT template.
KWC 446	PP7CP ORF_Fw2	CACCGGTCGCCACCATGCTAGCCTCCAAAAC CATCGTCTTTCGG	For amplification of PP7CP ORF for IVT template.
KWC 436	PP7CP ORF_Rv	GCCCCGCAGAAGGTCTAGACTAACGGCCCAG CGGCACAAG	For amplification of PP7CP ORF for IVT template.
KWC 430	U1Afull ORF_Fw	CACCGGTCGCCACCATGGCGGCAGTTCCCGA GACCCG	For amplification of U1A-full ORF for IVT template.
KWC 431	U1Afull ORF_Rv	GCCCCGCAGAAGGTCTAGACTACTTCTTGGC AAAGGAGATCTTCATG	For amplification of U1A-full ORF for IVT template.
KWC 405	EGFP mRNA1 ORF_Fw	CACCGGTCGCCACCATGGTGAGCAAGGGCGA G	For amplification of EGFP ORF for IVT template.
KWC 427	EGFP ORF_Rv	GCCCCGCAGAAGGTCTAGACTACTTGTACAG CTCGTCCATGCCGAGAG	For amplification of EGFP ORF for IVT template.
KWC 425	T7-5UTR for cassette1	TAATACGACTCACTATAGGTCAGATCCGCTA GCGGATCC	For amplification of 5'-UTR containing protein-binding motifs and EGFP ORF from switch plasmids.
KWC 433	T7-U1utr-EGFP_v2_fw	TAATACGACTCACTATAGACAGCATTGTACC CAGAGTCTGTCCCAGACATTGCACCTGGCG CTGTCCGAGATCGAGAAGAAGGCGAATTAA GAGAGAAAAGAAG	For amplification of IVT templates of U1utr-EGFP mRNA switches.
KWC 434	T7+g_Fw	CAGTGAATTGTAATACGACTCACTATAG	For amplification of IVT templates of mRNA switches.
YF771	T7_5UTR-fwd	ATTGTAATACGACTCACTATAGGGCGAATTA AGAGAGAAAAGAAGAGTAAG	For amplification of IVT template of iRFP670.
KD1-2	GCT7CMV_G	GCTAATACGACTCACTATAGGTCAGATCCGC TAGCG	For amplification of IVT templates of scMS2(WTx2)-EGFP mRNA switches.
HO3	T7_scMS2(WTx2)_fwd	GCTAATACGACTCACTATAGGGAGCAGGTGA GGATC	For amplification of 5'-UTR containing scMS2(WTx2) motif directly behind the 5'-end of mRNA.

**Table S6. Plasmids for generating synthetic mRNAs**

Name	Notes	Source
pScMS2(WTx2)-EGFP	For amplification of 5'-UTR that contains scMS2(WTx2) motif.	This study
pScPP7(2xWT)-EGFP	For amplification of 5'-UTR that contains scPP7(WTx2) motif.	This study
pMS2CP(V29I)-myc-T2A-tagRFP	Template plasmid for amplification of MS2CP(V29I) ORF.	This study
pPP7CP-myc-T2A-tagRFP	Template plasmid for amplification of PP7CP ORF.	This study
pU1A_full-myc-T2A-tagRFP	Template plasmid for amplification of U1A-full ORF.	This study
pUC19-iRFP670woT7f	Template plasmid for amplification of iRFP670 IVT template.	Gift from Dr. Fujita



**Table S7. Transfection tables of all experiments performed in this study**

Figure 1B-E, Figure S2

Switch plasmids	100 ng
Trigger/control plasmid	400 ng
Reference plasmid	100 ng
Opti-MEM	up to 100 $\mu$ L
Lipofectamine 2000	2 $\mu$ L

Figure 2, Figure S3

Switch plasmids	100 ng
Trigger/control plasmid	400 ng
Reference plasmid	100 ng
Opti-MEM	up to 100 $\mu$ L
Lipofectamine 2000	2 $\mu$ L

Figure 3, Figure S4 and S5

mRNA switch	100 ng	mRNAs were diluted in 5 $\mu$ L of nuclease-free water
Trigger mRNA	200 ng	
Reference mRNA	100 ng	
Opti-MEM	up to 50 $\mu$ L	
Lipofectamine MessengerMAX	1 $\mu$ L	

**Supplementary sequences**

EGFP, iRFP670, Protein binding motif, Scaffold sequence, Trigger ORF

**No aptamer**

GGGCGAAUUAAGAGAGAAAAGAAGAGUAAGAAGAAAUAUAAGACACCGGUCGCCACCAUGGUGAGCA  
AGGGCGAGGAGCUGUUCACCGGGGUGGUGCCCAUCCUGGUCGAGCUGGACGGCGACGUAACGGCCA  
CAAGUUCAGCGUGUCCGGCGAGGGCGAGGGCGAUGCCACCUACGGCAAGCUGACCCUGAAGUUAUC  
UGCACCACCGGCAAGCUGCCCUGGCCACCCUCGUGACCACCCUGACCUACGGCGUGCAGU  
GCUUCAGCCGCUACCCCGACCACAUGAAGCAGCAGACUUCUUAAGUCCGCCAUGCCCGAAGGCUA  
CGUCCAGGAGCGCACCAUCUUCUUAAGGACGACGGCAACUACAAGACCCGCGCCGAGGUGAAGUUC  
GAGGGCGACACCCUGGUGAACCGCAUCGAGCUGAAGGGCAUCGACUUAAGGAGGACGGCAACAUC  
UGGGGCACAAGCUGGAGUACAACUACAACAGCCACAACGUCUAUAUCAUGGCCGACAAGCAGAAGAA  
CGGCAUCAAGGUGAACUUAAGAUCGCGCCACAACAUUGAGGACGGCAGCGUGCAGCUCGCGGACCAC  
UACCAGCAGAACACCCCAUCGGCGACGGCCCGUGCUGCUGCCCGACAACCACUACCUGAGCACCC  
AGUCCGCCUGAGCAAAGACCCCAACGAGAAGCGCGAUCACAUGGUCCUGCUGGAGUUCGUGACCGC  
CGCCGGGAUCACUCUCGGCAUGGACGAGCUGUACAAGUAGUCUAGACCUUCUGCGGGGCUUGCCUUC  
UGGCAUGCCCUUCUUCUUCUCCUUGCACCUGUACCUCUUGGUCUUUGAAUAAAGCCUGAGUAGGAA  
AA  
AA

**iRFP670**

GGGCGAAUUAAGAGAGAAAAGAAGAGUAAGAAGAAAUAUAAGACACCGGUCGCCACCAUGGCGGUA  
AGGUCGAUCUCACCUCUGCGAUCGCGAGCCGAUCCACAUCCCCGCAGCAUUCAGCCGUGCGGCUG  
CCUGCUAGCCUGCGACGCGCAGGCGGUGCGGAUCACGCGCAUACGGAUUAACGGAUUAACGCGGCGUUCUU  
GGACGCGAAACUCCGCGGGUCGGUGAGCUACUCGCCGAUUAUCGCGGAGACCGAAGCCCAUGCGC  
UGCGCAACGCACUGGCGCAGUCCUCCGAUCCAAAGCGACCGGCGCUGAUCUUCGGUUGGCGGACGG  
CCUGACCGGCCGCACCUUCGACAUCUCACUGCAUCGCCAUGACGGUACAUCGAUCAUCGAGUUCGAG  
CCUGCGGGCGCCGAACAGGCCGACAAUCCGUGCGGCUGACGCGGAGAUCAUCGCGCGCACCAAAG  
AACUGAAGUCGCUCGAAGAGAUGGCCGCACGGGUGCCGCGCUAUCUGCAGGCGAUGCUCGGCUAUA  
CCGCGUGAUGUUGUACCGCUUCGCGGACGACGGCUCGCGGAUGGUGAUCGGCGAGGCGAAGCGCAGC  
GACCUCGAGAGCUUUCUGGUCAGCACUUUCGGCGUCGUGGUCGCGCAGCAGGCGGGCUACUGU  
ACUUGAAGAACGCGAUCGCGUGGUCUCGGAUUCGCGCGGAUCAGCAGCCGGAUCGUGCCCAGCA  
CGACGCCUCCGGCGCCGCGCUCGAUCUGUCGUUCGCGCACCUUGCGCAGCAUCUCGCCUUGCCAUCUC  
GAAUUUCGCGGAACAUGGGCGUCAGCGCCUCGAUGUCGUGCUGAUCAUCAUUGACGGCACGCUA  
GGGGAUUGAUAUCUGUCAUCAUUAACGAGCCGCGUGCCGUGCCGAUGGCGCAGCGGUCGCGGCCGA  
AAUGUUCGCCGACUUCUUAUCGCGCAGUUCACCGCCGCCACCACCAACGCAGAUCUCAUAUGCAU

CUCGAGUGAUAGUCUAGACCUUCUGCGGGGCUUGCCUUCUGGCCAUGCCCUUCUUCUCUCCCUUGCA  
CCUGUACCUCUUGGUCUUUGAAUAAAGCCUGAGUAGGAAAAAAAAAAAAAAAAAAAAAAAAAAAA  
AA  
AAAAAAAAAAAAAAAAAAAAAAAAAAAA

scMS2(WTx2)-EGFP

GGUCAGAUCCGCUAGCGGAUCCGGGAGCAGGUGAGGAUCACCCAUCUGCCACGAGCGAGGUGAGGAU  
CACCCAUCUCGCUCGUGUCCACC GGUCGCCACCAUGGUGAGCAAGGGCGAGGAGCUGUUCACCGG  
GGUGGUGCCCAUCCUGGUCGAGCUGGACGGCGACGUAAACGGCCACAAGUUCAGCGUGUCCGGCGAG  
GGCGAGGGCGAUGCCACCUACGGCAAGCUGACCCUGAAGUUCAUCUGCACCACCGGCAAGCUGCCCG  
UGCCUUGGCCACCCUCGUGACCACCCUGACCUACGGCGUGCAGUGCUUCAGCCGCUACCCCGACCA  
CAUGAAGCAGCACGACUUCUUAAGUCCGCCAUGCCGAAGGCUACGUCCAGGAGCGCACCAUCUUC  
UUCAAGGACGACGGCAACUACAAGACCCGCGCCGAGGUGAAGUUCGAGGGCGACACCUGGUGAACC  
GCAUCGAGCUGAAGGGCAUCGACUUAAGGAGGACGGCAACAUCUGGGGCACAAGCUGGAGUACAA  
CUACAACAGCCACAACGUCUAUAUCAUGGCCGACAAGCAGAAGAACGGCAUCAAGGUGAACUUCAAG  
AUCCGCCACAACAUCGAGGACGGCAGCGUGCAGCUCGCCACCACUACCAGCAGAACACCCCAUCG  
GCGACGGCCCCGUGCUGCUGCCCGACAACCACUACCUGAGCACCCAGUCCGCCUGAGCAAAGACCC  
CAACGAGAAGCGCGAUCACAUGGUCCUGCUGGAGUUCGUGACCGCCGCCGGGAUCACUCUCGGCAUG  
GACGAGCUGUACAAGUAGUCUAGACCUUCUGCGGGGCUUGCCUUCUGGCCAUGCCCUUCUUCUCC  
CUUGCACCUGUACCUCUUGGUCUUUGAAUAAAGCCUGAGUAGGAAAAAAAAAAAAAAAAAAAAAA  
AA  
AAAAAAAAAAAAAAAAAAAAAAAAAAAA

$\Delta$  spacer-scMS2(WTx2)-EGFP

GGGAGCAGGUGAGGAUCACCCAUCUGCCACGAGCGAGGUGAGGAUCACCCAUCUCGCUCGUGUCC  
ACCGGUCGCCACCAUGGUGAGCAAGGGCGAGGAGCUGUUCACCGGGGUGGUGCCCAUCCUGGUCGAG  
CUGGACGGCGACGUAAACGGCCACAAGUUCAGCGUGUCCGGCGAGGGCGAGGGCGAUGCCACCUACG  
GCAAGCUGACCCUGAAGUUCAUCUGCACCACCGGCAAGCUGCCCGUGCCUGGCCACCCUCGUGAC  
CACCCUGACCUACGGCGUGCAGUGCUUCAGCCGCUACCCCGACCACAUGAAGCAGCACGACUUCUUC  
AAGUCCGCCAUGCCCGAAGGCUACGUCCAGGAGCGCACCAUCUUCUUAAGGACGACGGCAACUACA  
AGACCCGCGCCGAGGUGAAGUUCGAGGGCGACACCUGGUGAACCGCAUCGAGCUGAAGGGCAUCGA  
CUUCAAGGAGGACGGCAACAUCUGGGGCACAAGCUGGAGUACAACUACAACAGCCACAACGUCUAU  
AUCAUGGCCGACAAGCAGAAGAACGGCAUCAAGGUGAACUUAAGAUCGCCACAACAUCGAGGACG  
GCAGCGUGCAGCUCGCCACCACUACCAGCAGAACACCCCAUCGGCGACGGCCCCGUGCUGCUGCC  
CGACAACCACUACCUGAGCACCCAGUCCGCCUGAGCAAAGACCCCAACGAGAAGCGCGAUCACAUG  
GUCCUGCUGGAGUUCGUGACCGCCGCCGGGAUCACUCUCGGCAUGGACGAGCUGUACAAGUAGUCUA

GACCUUCUGCGGGGCUUGCCUUCUGGCCAUGCCCUUCUUCUCUCCCUUGCACCUGUACCUCUUGGUC  
UUUGAAUAAAGCCUGAGUAGGAA  
AA  
AAAAAAA

scPP7(WTx2)-EGFP

GGUCAGAUCGCUAGCGGAUCCGGGAGCUAAGGAGUUUAUUGGAAACCCUUAGCCUGCUGCGUAAG  
GAGUUUAUUGGAAACCCUUACGCAGCAGUCCACCAGGUCGCCACCAUGGUGAGCAAGGGCGAGGA  
GCUGUUCACCGGGGUGGUGCCCAUCCUGGUCGAGCUGGACGGCGACGUAAACGGCCACAAGUUCAGC  
GUGUCCGGCGAGGGCGAGGGCGAUGCCACCUACGGCAAGCUGACCCUGAAGUUAUCUGCACCACCG  
GCAAGCUGCCCGUGCCUGGCCACCCUCGUGACCACCCUGACCUACGGCGUGCAGUGCUUCAGCCG  
CUACCCCGACCACAUGAAGCAGCAGACUUCUUAAGUCCGCAUGCCCGAAGGCUACGUCCAGGAG  
CGCACCAUCUUCUUAAGGACGACGGCAACUACAAGACCCGCGCCGAGGUGAAGUUCGAGGGCGACA  
CCUUGGUGAACCUGAUCGAGCUGAAGGGCAUCGACUUAAGGAGGACGGCAACAUCUGGGGCACAA  
GCUGGAGUACAACUACAACAGCCACAACGUCUAUAUCAUGGCCGACAAGCAGAAGAACGGCAUCAAG  
GUGAACUUAAGAUCGCGCACAAACUUCGAGGACGGCAGCGUGCAGCUCGCCGACCACUACCAGCAGA  
ACACCCCAUCGGCGACGGCCCCGUGCUGCUGCCGACAACCACUACCUGAGCACCAGUCCGCCCU  
GAGCAAAGACCCCAACGAGAAGCGGAUCACAUGGUCCUGCUGGAGUUCGUGACCGCCGCCGGGAUC  
ACUCUCGGCAUGGACGAGCUGUACAAGUAGUCUAGACCUUCUGCGGGGCUUGCCUUCUGGCCAUGCC  
CUUCUUCUCUCCCUUGCACCUGUACCUCUUGGUCUUUGAAUAAAGCCUGAGUAGGAAAAAAAAAAAA  
AA  
AA

U1utr-EGFP

GACAGCAUUGUACCCAGAGUCUGUCCCCAGACAUUGCACCUGGCGCUGUCCGAGAUCGAGAAGAAG  
GCGAAUUAAGAGAGAAAAGAAGAGUAAGAAGAAAUAUAAGACACCGGUCGCCACCAUGGUGAGCAAG  
GGCGAGGAGCUGUUCACCGGGGUGGUGCCCAUCCUGGUCGAGCUGGACGGCGACGUAAACGGCCACA  
AGUUCAGCGUGUCCGGCGAGGGCGAGGGCGAUGCCACCUACGGCAAGCUGACCCUGAAGUUAUCUG  
CACCACCGGCAAGCUGCCCGUGCCUGGCCACCCUCGUGACCACCCUGACCUACGGCGUGCAGUGC  
UUCAGCCGCUACCCCGACCACAUGAAGCAGCAGACUUCUUAAGUCCGCAUGCCCGAAGGCUACG  
UCCAGGAGCGCACCAUCUUCUUAAGGACGACGGCAACUACAAGACCCGCGCCGAGGUGAAGUUCGA  
GGGCGACACCUGGUGAACCUGAUCGAGCUGAAGGGCAUCGACUUAAGGAGGACGGCAACAUCUG  
GGCACAAGCUGGAGUACAACUACAACAGCCACAACGUCUAUAUCAUGGCCGACAAGCAGAAGAACG  
GCAUCAAGGUGAACUUAAGAUCGCGCACAAACUUCGAGGACGGCAGCGUGCAGCUCGCCGACCACUA  
CCAGCAGAACACCCCAUCGGCGACGGCCCCGUGCUGCUGCCCGACAACCACUACCUGAGCACCAG  
UCCGCCUGAGCAAAGACCCCAACGAGAAGCGGAUCACAUGGUCCUGCUGGAGUUCGUGACCGCCG



CCGGGAUCACUCUCGGCAUGGACGAGCUGUACAAGUAGUCUAGACCUUCUGCGGGGCUUGCCUUCUG  
GCCAUGCCCUUCUUCUCUCCCUUGCACCUGUACCUCUUGGUCUUUGAAUAAAGCCUGAGUAGGAAAA  
AA  
AA

**MS2CP(V29I)**

GGGCGAAUUAAGAGAGAAAAGAAGAGUAAGAAGAAAUAUAAGACACCGGUCGCCACC**AUGGCUUCUA**  
**ACUUUACUCAGUUCGUUCUCGUCGACAAUGGCGGAACUGGCGACGUGACUGUCGCCCAAGCAACU**  
**CGCUAACGGGAUCGCUGAAUGGAUCAGCUCUAAUCUCGCGAUCACAGGCUUACAAAGUAACCUGUAGC**  
**GUUCGUCAGAGCUCUGCGCAGAAUCGCAAUACACCAUCAAGUCGAGGUGCCUAAAGGCGCAUGGA**  
**GGUCUUACUUAAAUAUGGAACUAACCAUUCCAAUUUUCGCCACGAAUUCGACUGCGAGCUUAUUGU**  
**UAAGGCAAUGCAAGGUCUCCUAAAAGAUGGAAACCCGAUUCUCCUGGCAUCGCGGCAACUCCGGC**  
**AUCUACUGAAUCUAGACCUUCUGCGGGGCUUGCCUUCUGGCAUGCCCUUCUUCUCCCUUGCACC**  
UGUACCUCUUGGUCUUUGAAUAAAGCCUGAGUAGGAAAAAAAAAAAAAAAAAAAAAAAAAAAAAA  
AA  
AAAAAAAAAAAAAAAAAAAAAAAAAAAA

**PP7CP**

GGGCGAAUUAAGAGAGAAAAGAAGAGUAAGAAGAAAUAUAAGACACCGGUCGCCACC**AUGC****UAGCCU**  
**CCAAAACCAUCGUUCUUUCGGUCGGCGAGGCUACUCGCACUCUGACUGAGAUCAGUCCACCGCAGA**  
**CCGUCAGAUCUUCGAAGAGAAGGUCGGGCCUCUGGUGGGUCGGCUGCGCCUCACGGCUUCGCUCCGU**  
**CAAAACGGAGCCAAGACCGGUAUCGAGUCAACCUAAAACUGGAUCAGGCGGACGUCGUUGAUUCCG**  
**GACUCCGAAAGUGCGCUACACUCAGGUAUGGUCGCACGACGUGACAAUCGUUGCGAAUAGCACCGA**  
**GGCCUCGCGCAAUCGUUGUACGAUUUGACCAAGUCCUCGUCGCGACCUCGCAGGUCGAAGAUCUU**  
**GUCGUCAACCUUGUGCCCGUGGGCCGU**UAGUCUAGACCUUCUGCGGGGCUUGCCUUCUGGCAUGCC  
CUUCUUCUCUCCCUUGCACCUGUACCUCUUGGUCUUUGAAUAAAGCCUGAGUAGGAAAAAAAAAAAA  
AA  
AAAAAAAAAAAAAAAAAAAAAAAAAAAA

**U1A-full**

GGGCGAAUUAAGAGAGAAAAGAAGAGUAAGAAGAAAUAUAAGACACCGGUCGCCACC**AUGGcgGCAG**  
**UUCCCAGACCCGCCUAACCACACUAUUUAUAUCAACAACCUCAAUGAGAAGAUCAAGAAGGAUGA**  
**GCUAAAAAGUCCUGUACGCCAUUCUUCUCCAGUUUGGCCAGAUCUUGGAUAUCCUGGUAUCACGG**  
**AGCCUGAAGAUGAGGGGCCAGGCCUUUGUCAUCUUAAGGAGGUCAGCAGCGCCACCAACGCCUUCG**  
**GCUCCAUGCAGGGUUUCCCUUUCUAUGACAAACCUAUGCGUAUCCAGUAUGCCAAGACCGACUCAGA**  
**UAUCAUUGCCAAGAUGAAAGGCACCUUCGUGGAGCGGGACCGCAAGCGGGAGAAGAGGAAGCCCAAG**

